J. Neural Eng. **8** (2011) 025026 (6pp) doi:10.1088/1741-2560/8/2/025026

Analogue mouse pointer control via an online steady state visual evoked potential (SSVEP) brain–computer interface

John J Wilson and Ramaswamy Palaniappan

Brain-Computer Interface Group, School of Computer Science and Electronic Engineering, University of Essex, Wivenhoe Park, Colchester, CO4 3SQ, Essex, UK

E-mail: jjwils@essex.ac.uk and rpalan@essex.ac.uk

Received 26 July 2010
Accepted for publication 23 November 2010
Published 24 March 2011
Online at stacks.iop.org/JNE/8/025026

Abstract
The steady state visual evoked protocol has recently become a popular paradigm in brain–computer interface (BCI) applications. Typically (regardless of function) these applications offer the user a binary selection of targets that perform correspondingly discrete actions. Such discrete control systems are appropriate for applications that are inherently isolated in nature, such as selecting numbers from a keypad to be dialled or letters from an alphabet to be spelled. However motivation exists for users to employ proportional control methods in intrinsically analogue tasks such as the movement of a mouse pointer. This paper introduces an online BCI in which control of a mouse pointer is directly proportional to a user's intent. Performance is measured over a series of pointer movement tasks and compared to the traditional discrete output approach. Analogue control allowed subjects to move the pointer faster to the cued target location compared to discrete output but suffers more undesired movements overall. Best performance is achieved when combining the threshold to movement of traditional discrete techniques with the range of movement offered by proportional control.

1. Introduction

The steady state visual evoked potential (SSVEP) has proved a popular paradigm for a brain–computer interface (BCI) due to its robust presence in electroencephalogram (EEG) signals. The SSVEP is evoked when a subject is exposed to repeated visual stimulation such that the reaction to a subsequent stimulus occurs before the effect of the previous stimulus has subsided (Regan 1989). An SSVEP BCI is normally constructed by presenting the user with multiple stimuli that are distinct in repetition rates. Previous SSVEP BCIs have used stimuli repeating in the range 6–60 Hz (Vialatte *et al* 2010). Each stimulus is typically tagged to a specific command or action that the user is able to perform. Stimuli can be presented through use of flashing light-emitting diodes (LEDs) or alternatively standard CRT or LCD monitors can be employed to output a variety of stimuli through computer-generated imagery (CGI). However, this type of presentation is severely limited in the number of distinct stimuli that do not suffer from temporal aliasing due to the comparatively low refresh rate (60–120 Hz) of typical standard visual display units (Bach *et al* 1997, Volosyak *et al* 2009a). Nevertheless, a significant benefit of CGI is that stimuli can be integrated and manipulated within the BCI display environment far more easily than hardware stimulators such as LEDs.

Typically, past SSVEP BCIs have determined a user's intent or gaze through frequency spectrum analysis of the EEG signal (Middendorf *et al* 2000) (Gao *et al* 2003, Cheng *et al* 2002, Kelly *et al* 2005, Müller-Putz *et al* 2005, Wang *et al* 2006). This is most commonly implemented using the Fourier transform, particularly the fast Fourier transform (FFT). FFT EEG epochs ranging from four to eight seconds are typically employed. Larger epoch lengths provide two benefits. Firstly, there is increased spectral resolution, aiding successful discrimination of stimuli in the system. Interfaces with up to 48 targets separated by just 0.2 Hz have been presented (Gao *et al* 2003). Secondly, increasing the signal-to-noise ratio within an EEG epoch, as the FFT operation, is in itself an average of the power of individual stimuli flash cycles. However, increased epoch lengths come at the expense of time

Figure 1. Screenshot of the stimulator/pointer engine at the start of a 'left movement' task, having just successfully completed an 'up-movement' task. Screen resolution: 1920 × 1080. Pointer reticule (upper-right part of figure): 150 × 150. Stimuli gratings (surrounding reticule): 200 × 50/50 × 200. 15 Hz: down/bottom. 12 Hz: left. 10 Hz: top/up. 8.57 Hz: right. Target icon (upper-left part of figure): 25 × 25, situated 200 pixels from top and left edge.

taken to collect the EEG resulting in a performance trade-off between accuracy and time when calculating the information transfer rate (ITR) of a system.

Less well explored is performing the FFT operation on much reduced epoch sizes such as a single-cycle basis (EEG epoch lengths that encompass a single flash or stimulation event). This technique allows us to gain a notion of the contribution of each flash (in amplitude and phase) to larger epoch FFT averages. Single-cycle analysis also allows use of standard significance tests to classify the presence of SSVEP, allowing confidence criteria to be set across all subjects, negating the need for a training phase or setting of thresholds by empirical measurement on a per subject basis (Wilson and Palaniappan 2009).

To the authors' knowledge only four published online SSVEP BCIs have involved controlling movement as opposed to making discrete selections from a keypad or alphabet etc (Lalor *et al* 2005, Martinez *et al* 2007, Muller-Putz and Pfurtscheller 2008, Trejo *et al* 2006). In all of the above cases the output of the system is binary, i.e. a yes/no decision is made and the resulting action is discrete in nature.

This paper will demonstrate that by examining EEG on a single-cycle basis, features can be extracted to provide feedback that can represent a range of values proportional to a user's intent, rather than an on–off thresholded switch approach. We introduce a four-class pointer control BCI which operates in three distinct control modes. The first, 'discrete mode', is akin to the examples mentioned above in that if after the analysis of EEG a criterion is met, the output is a one pixel movement of the pointer. In the second, 'analogue mode', at no time is a yes/no binary decision made, the movement of the pointer is directly proportional to the intention of the user. Finally 'combined mode' uses both the thresholding criteria of 'discrete mode' and the output of 'analogue mode' together. Six subjects completed a series of pointer movement tasks using this online system to facilitate comparisons of each control mode in terms of time and accuracy.

2. Methods

2.1. Subjects

Six healthy right-handed adults (four males, two females) with normal or corrected-to-normal vision participated in the study, aged 18–54 (mean age 34). All subjects were naïve to BCI experiments. Each subject completed the entire experiment in a normal office environment within the BCI Group at the University of Essex and received no remuneration.

2.2. Stimulator/pointer engine

The stimulator/pointer engine (figure 1) was displayed to each subject using a standard widescreen flat panel LCD monitor at a standard HD resolution of 1920 × 1080 with a refresh rate of 60 Hz. Each subject was situated at a distance of 60 cm from the screen with the bottom edge at eye level. During an active trial displayed on the screen was a pointer reticule surrounded by four colour reversing gratings serving as SSVEP targets. Each grating was distinct in reversal rates and located around the reticule corresponding to the four directions the user was able to move the reticule. In keeping with our previous research (Wilson and Palaniappan 2009), the target frequencies were 15, 12, 10 and 8.57 Hz, corresponding to integer divisors of the 60 Hz screen refresh rate. The user was able to move the reticule around the screen by simply attending the stimulus corresponding to the direction they wished the reticule to move.

2.3. EEG acquisition

EEG was recorded using three gold electrodes, two in a bipolar configuration at locations Oz and PO3 according to the international 10/20 system and a final electrode at the forehead (Fpz) serving as ground. Impedances were kept below 5 Ω through use of conductive paste. The EEG biosignal amplifier employed was the g.BS*amp* coupled to the g.16*sys* subsystem (g.tec, Guger Technologies) incorporating a hardware bandpass from 2 to 30 Hz, with a notch filter at 50 Hz (UK ac power frequency). The sampling rate was $Fs = 300$ Hz to provide an integer number of points encompassing each stimulus single cycle. This allows the frequencies of interest to be fully contained within an individual FFT 'bin' alleviating spectral leakage (Bach and Meigen 1999).

2.4. Signal processing and single-cycle extraction

Initially a four second (1200 samples) epoch of EEG was collected. Rectangular sliding windows corresponding to single cycle sample lengths of the four stimuli (20pts—15 Hz, 25pts—12 Hz, 30pts—10 Hz, 35pts—8.57 Hz) were sequentially slid over the epoch and submitted to an FFT operation individually. The resulting arrays of complex components from 'Bin 1' corresponding to each of the four stimuli fundamental repetition rates were then passed to each control mode analysis engine simultaneously. The epoch was then updated by five samples on a first in first out (FIFO) basis and the sliding windows and the FFT process repeated. This equated to a fundamental system speed of 60 Hz ($Fs = 300/5$), meaning a decision was made by the system to move the pointer every 16.66 ms.

2.5. Discrete classification

Each array of computed single-cycle Fourier complex components $F(n)$ and their means $\langle F(n)\rangle_{\text{est}}$ extracted from the four distinct window lengths corresponding to each stimulus were simultaneously submitted to a circular T^2-test $\left(T^2_{\text{circ}}\right)$ (Victor and Mast 1991):

$$T^2_{\text{circ}} = (N-1)\frac{|\langle F(n)\rangle_{\text{est}} - \mu|^2}{\sum_{n=1}^{N} |F(n) - \langle F(n)\rangle_{\text{est}}|^2}. \tag{1}$$

Equation (1) defines the T^2_{circ} statistic and shows that for N independent estimates of $F(n)$ drawn from a sample of assumed mean of $\mu = 0$ (no SSVEP response or noise), $N.T^2_{\text{circ}}$ is distributed according to $F_{[2,2N-2]}$. The basic application of the T^2_{circ} statistic is the determination of whether an observed set of Fourier components is consistent with random fluctuations alone (EEG noise), or conversely, whether this set of observations implies (to within a given confidence level) that an SSVEP component is present. The T^2_{circ} confidence level was set at 1%; values of p falling below this level ($p < 0.01$) resulted in a pointer movement of 1 pixel in the direction represented by the array of Fourier components that had reached significance.

2.6. Analogue classification

$$\text{PLI} = \left| \frac{1}{N} \sum_{n=1}^{N} \frac{F(n)}{|F(n)|} \right|. \tag{2}$$

Simultaneously, each $F(n)$ was also normalized and compared purely on its phase component using equation (2) (Rayleigh 1880, Stapells *et al* 1987). This produced a phase locking index (PLI) score ranging from 0 to 1 with a value of 1 indicating a completely phase coherent response (all cycles have exact phase) and zero indicating a completely incoherent response with cycles having phase equally spread about 360°. The PLI value was subsequently scaled by a factor of 5 and the resulting value the distance in pixels to be moved in the corresponding direction by the pointer, thus giving a range of pointer movement values possible from 0 to 5 pixels.

2.7. Combined mode

Combined mode uses aspects of both the previous discrete and analogue modes. Initially it is identical to discrete mode in that a pointer movement only occurs if the T^2_{circ} statistic is significant; however, when this condition is met, instead of a pointer movement of a single pixel a movement of distance equivalent to that calculated by the PLI value in the analogue mode method is used instead.

2.8. Experimental setup

Each subject was required to complete two trials consisting of four distinct left, right, up and down pointer movement tasks over all three control modes, thus completing six trials and 24 pointer movement tasks in total (see figure 2 for description). Each movement task required the subject to move the pointer reticule over a laterally placed target icon. Therefore to successfully 'hit' a target only a single plane directional movement was required from the reticule initial position or after successfully hitting a previous target. However, all stimuli were active at all times and subjects were free to choose a trajectory of their choice and indeed would need to command two-dimensional movements to correct undesired orthogonal movements away from the target icon. Note that as analysis of all stimuli occurred simultaneously it was entirely possible that combined movements such as diagonal direction could be achieved.

The pointer reticule was confined to the edges of the screen but each target icon was located so a subject was unable to 'drag' along the edge of the screen to complete the movement task. The order in which control modes were employed for each trial was block arranged across the six subjects, meaning all subjects completed each trial in a unique order with respect to control modes. The trajectory of the centre of the reticule pointer and elapsed time were recorded for performance analysis for each task in each trial. An accuracy statistic was derived from the output of the BCI at each movement decision step. If the location of the pointer was a greater distance from the target (in either horizontal or vertical plane) than in the previous step then the previous output was classed as a 'undesired move'.

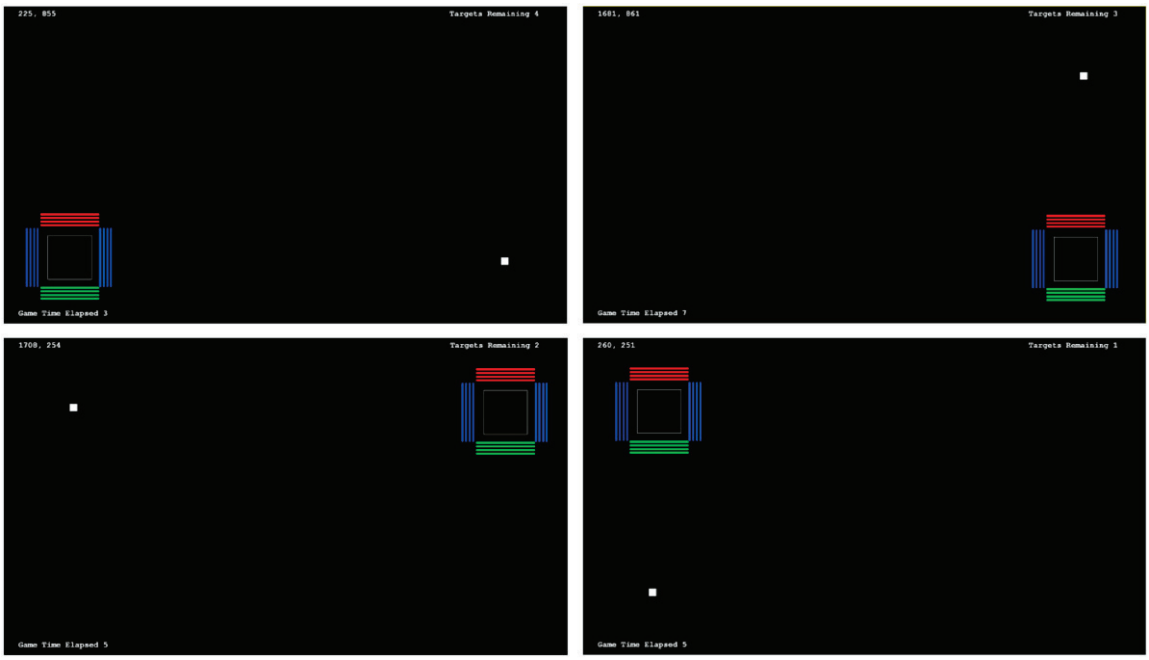

Figure 2. Order of movement tasks for trial 1. Movement task 1 (upper left). Movement task 2 (upper right). Movement task 3 (lower left). Movement task 4 (lower right). In trial 2 movement tasks were reversed. The pointer reticule was initially located 20 pixels from the edges of the left corner of the screen at the start of trial 1 and of the right corner for trial 2. In every movement task the target icon was located 200 pixels from the edges of the respective corners.

Table 1. Grand average completion times (s) across all movements.

Movement	Frequency	Discrete*	Analogue^	Combined+	All
Right	8.57 Hz	29.91	29.07	13.39*,^	20.23
Up	10 Hz	24.53	19.18	14.59*	17.07
Left	12 Hz	45.30^	54.36	36.55^	37.05
Down	15 Hz	23.99	36.25	20.57^	23.95
All		30.93	34.71	21.28	

*,^,+denote that time taken is significantly less than discrete, analogue or combined respectively (paired t-test, one-tailed, $p < 0.05$).

Table 2. Grand average undesired move percentages (%) across all movements.

Movement	Frequency	Discrete*	Analogue^	Combined+	All
Right	8.57 Hz	3.06^	19.52	7.85^	10.14
Up	10 Hz	1.28^	13.68	5.85^	6.93
Left	12 Hz	5.95^	18.04	6.25^	10.08
Down	15 Hz	3.54^	10.39	2.57^	5.50
All		3.45	15.40	5.63	8.16

*,^,+denote that the result is significantly less than discrete, analogue or combined respectively (paired t-test, one-tailed, $p < 0.05$).

3. Results

Table 1 depicts the average completion times for each movement task over all subjects and trials in addition to the grand averages over all movements and all control modes. The combined mode was significantly faster ($p < 0.05$) than either the discrete or the analogue mode for all movement tasks. There was only a significant difference between analogue and discrete mode completion times during the left movement task.

Table 2 depicts the average percentage of wrong moves for each movement task over all subjects and trials in addition to the grand averages over all movements and all control modes. Higher values represent pointer trajectories that were less accurate. The discrete and combined modes were statistically significantly more accurate than the analogue mode for all movement tasks. There was no significant difference in accuracy between the discrete and combined modes.

4. Discussion

It is apparent that the lower threshold to movement of the PLI algorithm incorporated in the analogue mode is more susceptible to noise (contamination from other stimuli or by ongoing brain rhythms overlapping with stimuli frequencies) compared to the robust statistical test of discrete mode. This resulted in any time saved in moving the pointer in larger individual steps being lost in correcting unwanted movements. Additionally, the discrete mode retains both phase and amplitude information in calculation of the T^2_{circ} statistic compared to analogue mode which disregards amplitude, classifying SSVEP purely on the phase coherence of the single-cycle vectors around the unit circle. Thus PLI is not an optimum basis for classification of SSVEP alone because individual amplitudes of stimuli flash events and noise are unlikely to be equal. It is also interesting to note that the highest percentage of wrong moves in the analogue mode occurred from the target stimuli encompassing the alpha EEG

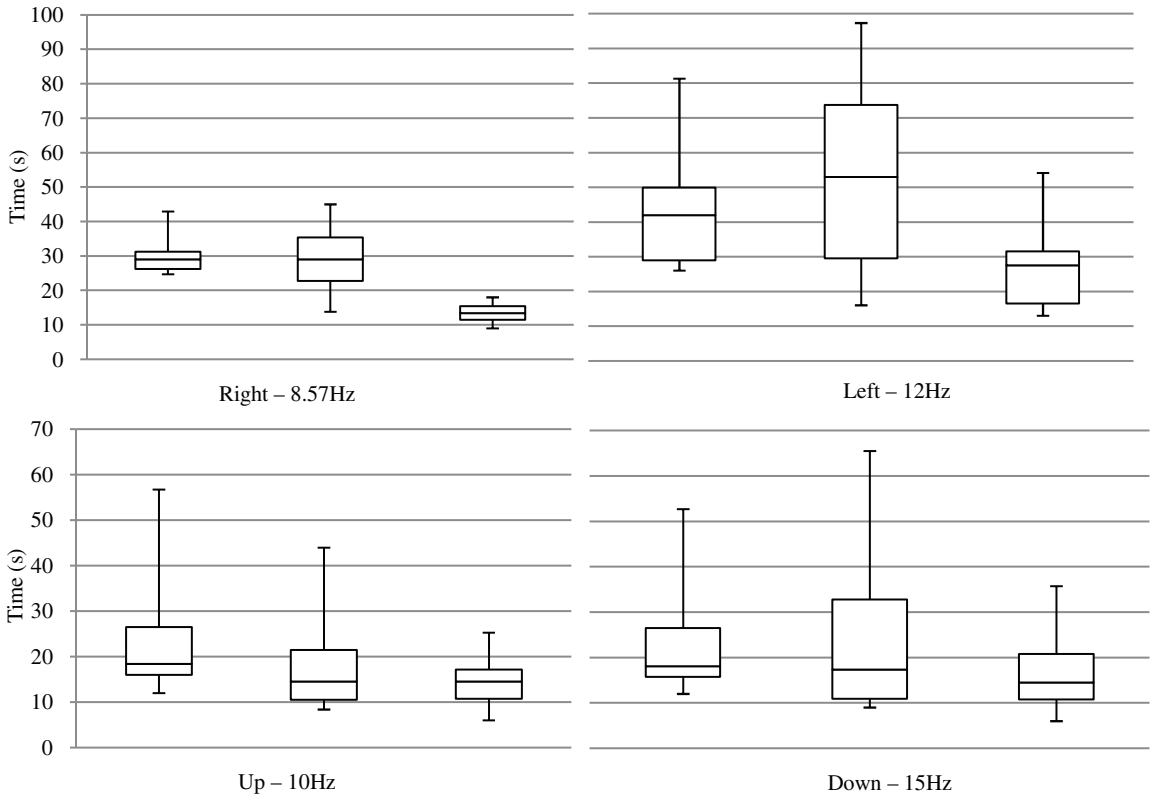

Figure 3. Range of completion times for each movement task across all subjects. In each instance: left plot—discrete mode; centre plot—analogue mode; right plot—combined mode.

region 8–12 Hz, whereas the higher 15 Hz tagged stimulus suffered from the least percentage of wrong moves reinforcing this theory. Completion times while using analogue control also had the largest interquartile range over all movement tasks (figure 3). Some subjects were better able to control the higher sensitivity of analogue control compared to others or perhaps suffered from less spontaneous alpha contamination. Movement direction tasks employing the lower frequency targets in each plane had tighter distributions compared to the opposing movement higher frequency targets with the tightest distribution being at the lowest frequency of 8.57 Hz. These results are in harmony with the Bremen-BCI, which was tested with 37 subjects (Volosyak *et al* 2009b).

The discrete mode suffered the smallest percentage of wrong moves over all modes because in addition to utilising both amplitude and phase information, any unwanted movement, no matter how severe the contamination, could only result in a single pixel movement in the wrong direction. The subject was therefore able to take corrective action before the pointer moved too far in an undesired direction.

The combined mode, as expected, benefits from the more robust classification of discrete control and proportional movement range of analogue control, resulting in significantly faster performance than the discrete or analogue modes, with no significant loss in accuracy over discrete control.

It is important to note that the times reported in table 1 could be improved by simply scaling the output of all the control modes by a constant factor to increase the distance the pointer moves at each step. However, in doing so the granularity of movement would be degregated. All control modes in this BCI are able to move the pointer with a granularity of a single pixel. This guarantees the system to be operable with any end user application as in any hypothetical system targets must be separated by at least 1 pixel to indeed be separable. Of course, typically targets are much larger than this in real-world applications, e.g. a standard Microsoft Windows icon is 32 × 32 pixels. In addition, if applying this BCI to current operating system environments a 'wrap around' feature of the pointer could be implemented, i.e. as the user travels to the edge of the screen they continue until they reappear at the opposite edge.

Performance quantization of online asynchronous BCIs through traditional ITR calculations is troublesome due to the fact that the system is asynchronous in the sense that the user decides which stimuli to attend and when, as opposed to a cue-based offline system. Performance quantization of pointer movement is even more problematic in that movement even with a traditional human–computer interface such as a mouse is inherently fuzzy. For example, a user does not always move the pointer on the most efficient route, especially when the target of interest is not located laterally. Thus we have turned to real-world efficiency measures to quantify the performance of the BCI in time taken to complete a goal and classing accuracy in terms of movements away from the target (whether desired or not) as opposed to restricting the system and tasks to be able to calculate an ITR.

5. Conclusion

This work has demonstrated effective techniques that can be employed to provide analogue or proportional control in an online SSVEP BCI. In any online BCI there is a relationship between the user input and BCI output; any additional control that can be provided and evidence of the control being utilized in feedback to the user will result in a better harmony using the system and in turn better results. It is important to always relate the output of the BCI to the application at hand. An additional stimulus target could be added or eye blink incorporated to operate as a mouse 'click' or select function in the presented BCI. The system could then be employed in a current Windows OS environment whereby the control mode is determined by the location of the pointer within the interface. For example, when the pointer is over the scroll bar the discrete mode is employed because the cursor must remain relatively stationary on the x axis and move consistently up or down the y axis. When the pointer is on the desktop and the user is searching for an icon, the analogue or the combined mode could be employed. In this way, the control of the BCI can be designed to fit the demands of the application in addition to augmenting applications to fit the BCI.

Acknowledgment

The first author would like to thank the EPSRC for funding his PhD via the Doctoral Training Grant.

References

Bach M and Meigen T 1999 Do's and don'ts in Fourier analysis of steady-state potentials *Doc. Ophthalmol.* **99** 69–82

Bach M, Meigen T and Strasburger H 1997 Raster-scan cathode-ray tubes for vision research-limits of resolution in space, time and intensity, and some solutions *Spat. Vis.* **10** 403–14

Cheng M, Gao X, Gao S and Xu D 2002 Design and implementation of a brain-computer interface with high transfer rates *IEEE Trans. Biomed. Eng.* **49** 1181–6

Gao X, Xu D, Cheng M and Gao S 2003 A BCI-based environmental controller for the motion-disabled *IEEE Trans. Neural Syst. Rehabil. Eng.* **11** 137–40

Kelly S P, Lalor E C, Reilly R B and Foxe J J 2005 Visual spatial attention tracking using high-density SSVEP data for independent brain–computer communication *IEEE Trans. Neural Syst. Rehabil. Eng.* **13** 172–8

Lalor E C, Kelly S P, Finucane C, Burke R, Smith R, Reilly R B and McDarby G 2005 Steady-state VEP-based brain-computer interface control in an immersive 3D gaming environment *EURASIP J. Adv. Signal Process.* **19** 3156–64

Martinez P, Bakardjian H and Cichocki A 2007 Fully online multicommand brain-computer interface with visual neurofeedback using SSVEP paradigm *Comput. Intell. Neurosci.* **2007** 94561

Middendorf M, McMillan G, Calhoun G and Jones K S 2000 Brain-computer interfaces based on the steady-state visual-evoked response *IEEE Trans. Rehabil. Eng.* **8** 211–4

Muller-Putz G R and Pfurtscheller G 2008 Control of an electrical prosthesis with an SSVEP-based BCI *IEEE Trans. Biomed. Eng.* **55** 361–4

Müller-Putz G R, Scherer R, Brauneis C and Pfurtscheller G 2005 Steady-state visual evoked potential (SSVEP)-based communication: impact of harmonic frequency components *J. Neural Eng.* **2** 123

Rayleigh L 1880 On the resultant of a large number of vibrations of the same pitch and of arbitrary phase *Phil. Mag.* **10** 73–8 Series 5

Regan D 1989 *Human Brain Electrophysiology: Evoked Potentials and Evoked Magnetic Fields in Science and Medicine* (New York: Elsevier)

Stapells D R, Makeig S and Galambos R 1987 Auditory steady-state responses: threshold prediction using phase coherence *Electroencephalogr. Clin. Neurophysiol.* **67** 260–70

Trejo L J, Rosipal R and Matthews B 2006 Brain-computer interfaces for 1-D and 2-D cursor control: designs using volitional control of the EEG spectrum or steady-state visual evoked potentials *IEEE Trans. Neural Syst. Rehabil. Eng.* **14** 225–9

Vialatte F-B, Maurice M, Dauwels J and Cichocki A 2010 Steady-state visually evoked potentials: Focus on essential paradigms and future perspectives *Prog. Neurobiol.* **90** 418–38

Victor J D and Mast J 1991 A new statistic for steady-state evoked potentials *Electroencephalogr. Clin. Neurophysiol.* **78** 378–88

Volosyak I, Cecotti H and Graser A 2009a Impact of frequency selection on LCD screens for SSVEP-based brain-computer interfaces *Proc. 10th Int. Work-Conf. on Artificial Neural Networks: Part I. Bio-Inspired Systems: Computational and Ambient Intelligence* ed J Cabestany, F Sandoval, A Prieto and J M Corchado *Lecture Notes in Computer Science* 5517 (Berlin: Springer) pp 706–13

Volosyak I, Cecotti H and Graser A 2009b Optimal visual stimuli on LCD screens for SSVEP based brain-computer interfaces *Proc. 4th Int. IEEE/EMBS Conf. on Neural Engineering* pp 447–50

Wang Y, Wang R, Gao X, Hong B and Gao S 2006 A practical VEP-based brain–computer interface *IEEE Trans. Neural Syst. Rehabil. Eng.* **14** 234–9

Wilson J J and Palaniappan R 2009 Augmenting a SSVEP BCI through single cycle analysis and phase weighting *Proc. 4th Int. IEEE/EMBS Conf. on Neural Engineering* pp 371–4